Supporting Information

Boosting Water Oxidation Electrocatalysts with Surface Engineered Amorphous Cobalt Hydroxide Nanoflakes

Haoxuan Zhang,[a] Bingxu Chen,[b] Hao Jiang,*[a] Xuezhi Duan,[b] Yihua Zhu,[a] Chunzhong Li*[a]

[a.] Key Laboratory for Ultrafine Materials of Ministry of Education, School of Materials Science and Engineering, East China University of Science and Technology, Shanghai 200237, China

[b.] State Key Laboratory of Chemical Engineering and Department of Chemical Engineering, East China University of Science and Technology, Shanghai 200237, China

*Corresponding author: Tel.: +86-21-64250949, Fax: +86-21-64250624

E-mail: jianghao@ecust.edu.cn (Prof. H. Jiang) czli@ecust.edu.cn (Prof. C. Z. Li)

Part I: Experimental Section

1.1 Synthesis of $Co(OH)_xS$ nanoflakes:

Commercial Ni foam (0.6 cm × 0.5 cm × 0.3 mm) was immersed in 3 M HCl for 15 minutes to remove surface oxides before use. And a two-electrode system was built with a cleaned nickel foam as working electrode, a graphite bar as both counter and reference electrode, and 30 mL aqueous solution containing $Co(NO_3)_2 \cdot 6H_2O$ (1.5 mmol) and C_2H_5NS (4.5 mmol) as electrolyte. The electrodeposition process was performed on Ni foam by repeated current-polarity switching strategy. Typically, a current of -5 mA was firstly applied using a galvanostatic method for 200 s, and then switched to 3 mA for 250 s. After this process was repeated four times, the $Co_1(OH)_xS_1$ nanoflakes have been obtained. The S/Co ratio can be conveniently regulated by changing the anodic deposition time, *e.g.* $Co(OH)_xS_{0.6}$ (150 s) and $Co(OH)_xS_2$ (350 s). In addition, pure $Co(OH)_x$ nanoflakes were also synthesized for comparison using a current of -5 mA for 800 s in 0.0015 M $Co(NO_3)_2 \cdot 6H_2O$ solution (30 mL).

1.2 Characterization:

The structure and morphology of the as-obtained samples were characterized by X-ray powder diffraction (XRD; Rigaku D/Max 2550, Cu Kα radiation) at a scan rate of 1° min^{-1}, field-emission scanning electron microscopy (FESEM, Hitachi, S-4800, 15 kV), transmission electron microscopy (TEM; JEOL, JEM-2100F) with an X-ray energy dispersive spectrometer (EDS) and an electron energy loss spectroscopy (EELS) at an accelerating voltage of 200 kV, and X-ray photoelectron spectroscopy (XPS; Thermal Scientific, EscaLab 250Xi). Inductively coupled plasma mass spectrometry (ICP-MS) was performed by an Agilient 7700 spectrometer.

1.3 Electrochemical Measurements:

The electrochemical measurements were performed in a standard three-electrode system connected to an electrochemical workstation (CHI 660E) with a saturated Ag/AgCl reference electrode and a graphite counter electrode. The electrocatalysts supported on Ni foam were directly used as a working electrode. The loading mass of electrocatalysts on Ni foam is about 1.0 mg cm^{-2}. All potentials measured were calibrated to reversible hydrogen electrode (RHE) by the following equation:

$$E_{RHE} = E_{Ag/Agcl} + 0.1976 + 0.0591 \times pH$$

All measurements were performed in 1.0 M KOH aqueous solution under gently stirring to get rid of bubbles. Before the electrochemical measurements, the electrolyte was purged with O_2 for at least 30 minutes to achieve an O_2-saturated condition. The electrocatalysts were activated in advance at a current density of 10 mA cm^{-2} until the voltage keeps unchanged. Linear sweep voltammetry at sweep rate of 1 mV s^{-1} and chronopotentiometry were performed with 95 % *iR* drop compensation. Electrochemical impedance spectroscopy (EIS) was performed by a three-electrode cell system in frequency range from 10 kHz to 100 mHz. The turnover frequency (TOF) was calculated by the following equation:

$$TOF = \frac{J \times A}{2 \times F \times \mathrm{n}}$$

where *J* is the current density in the LSV curves, *A* is the geometric area of electrode, *F* is the Faraday constant (C mol^{-1}), and *n* is the mole number of active sites on the electrode. The Co contents are 0.0014, 0.0017, 0.0019 and 0.0010 mmol in $Co(OH)_xS_{0.6}$, $Co(OH)_xS$, $Co(OH)_xS_2$ and $Co(OH)_x$ samples, respectively, based on the inductively coupled plasma mass spectrometry (ICP-MS) results. As comparisons, the $Co(OH)_x$ nanoflakes, the $Co(OH)_xS$ nanoflakes aggregation and the commercial RuO_2 powders supported on Ni foam (loading mass = 1.0 mg cm^{-2}) were respectively measured for OER performance.

1.4 DFT Calculations:

All periodic spin-polarized DFT calculations were performed using the Vienna ab initio simulation package (VASP).[S1-S3] The interactions between ion cores and valence electrons were described by the projector augmented wave (PAW) method, and the exchange-correlation energy of the electrons was obtained within the GGA-DFT plus Hubbard-U framework, which has been shown to improve the description of cobalt oxides, and the value of (U-J) equal to U_{eff} = 3.52 eV was used throughout this work according to previous studies.[S4-S8] The solution of the Kohn-Sham equations was expanded in a plane wave basis set with a cutoff energy of 400 eV. The Brillouin zone sampling was performed using a Monkhorst-Pack grid, and electronic occupancies were determined in light of a Methfessel-Paxton scheme with an energy smearing of 0.2 eV.[S9-S10] In all the calculations, a force-based conjugated gradient method was used to optimize the geometries.[S11] Saddle points and minima were considered to be converged when the maximum force in each degree of freedom was less than 0.03 eV $Å^{-1}$. Atomic charges were calculated based on the method due to Bader with the algorithms developed by Henkelman *et al.*, and the core charge density was included in the partitioning.[S12,S13]

In alkaline media, the oxygen evolution reaction (OER) can proceed through a four-electron reaction, which can be written as following elementary steps:

$$OH^- + * \rightarrow HO* + e^- \qquad \text{(S1)}$$

$$OH* + OH^- \rightarrow O* + H_2O + e^- \qquad \text{(S2)}$$

$$O* + OH^- \rightarrow HOO* + e^- \qquad \text{(S3)}$$

$$HOO* + OH^- \rightarrow H_2O + O_2 + e^- \qquad \text{(S4)}$$

where * stands for OER active sites, and *HO**, *O**, *HOO** are absorbed intermediates. The overpotentials of OER can be determined by computing the free energies of the different elementary steps, which is defined as the difference between free energies of the initial and final states for each steps, and can be given by the following equation:

$$\Delta G = \Delta E + \Delta ZPE - T\Delta S + \Delta G_U + \Delta G_{pH} \qquad \text{(S5)}$$

where ΔE is the reaction energy of reactants and products adsorbed on catalyst surface, ΔZPE is the change of zero-point energy, T is the temperature, ΔS is the entropy change at 298.15K, $\Delta G_U = -eU$ (U is the electrode potential and e is the transferred charge), and ΔG_{pH} is the correction of the H^+ free energy. The overpotential can be calculated by the following equations:

$$\Delta G_{OER} = \max\{\Delta G_1, \Delta G_2, \Delta G_3, \Delta G_4\} \qquad \text{(S6)}$$

$$\eta^{OER} = \max\frac{\{\Delta G_1, \Delta G_2, \Delta G_3, \Delta G_4\}}{e} - 1.23 \qquad \text{(S7)}$$

Structure of CoOOH is calculated and the corresponding lattice parameters (*i.e.*, a = 2.84 Å, b = 13.00 Å) are in accordance with previous experimental and theoretical results.[S8] We cleaved the (0001) surface of the CoOOH with the cell size of 2 × 2 primitive cell and vacuum thickness of 10 Å. To mimic sulfur engineered CoOOH layer, sulfur atoms were absorbed on the CoOOH (0001) surface as the computational model.

Part II: Supporting Figures

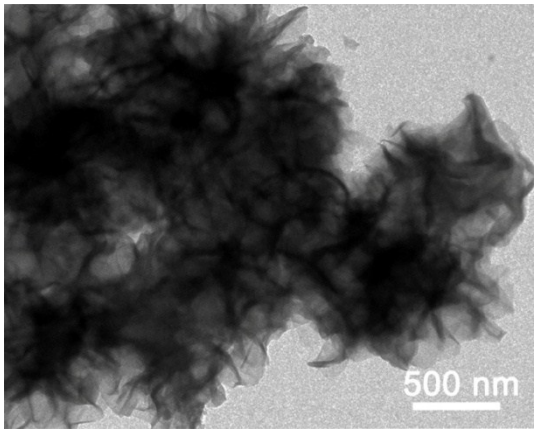

Fig. S1 TEM image of $Co(OH)_xS$ nanoflakes.

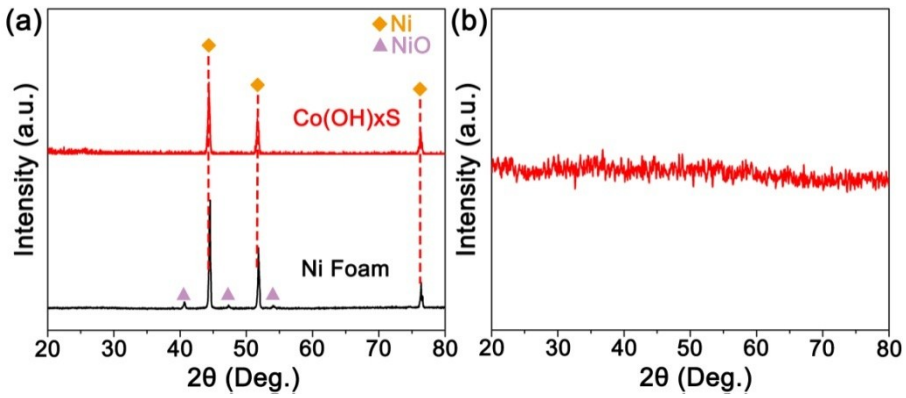

Fig. S2 XRD patterns of $Co(OH)_xS$ nanoflakes (a) on Ni foam and (b) as powder sample.

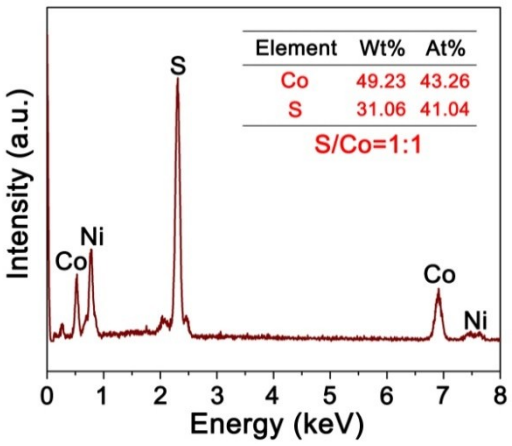

Fig. S3 EDS spectrum of $Co(OH)_xS$ nanoflakes.

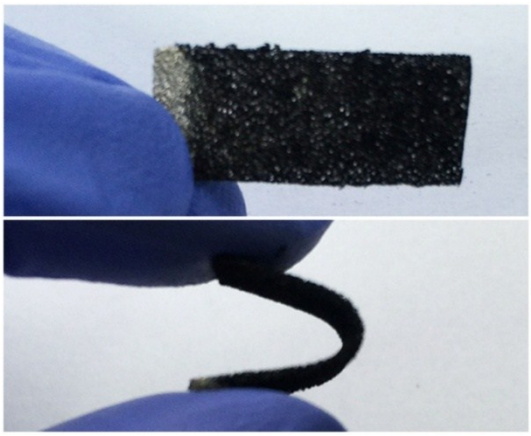

Fig. S4 Digital photographs of $Co(OH)_xS$ nanoflakes in flat and bending state.

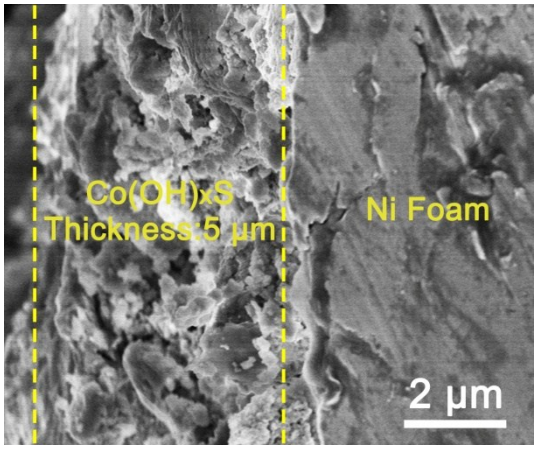

Fig. S5 Sectional SEM image of $Co(OH)_xS$ nanoflakes.

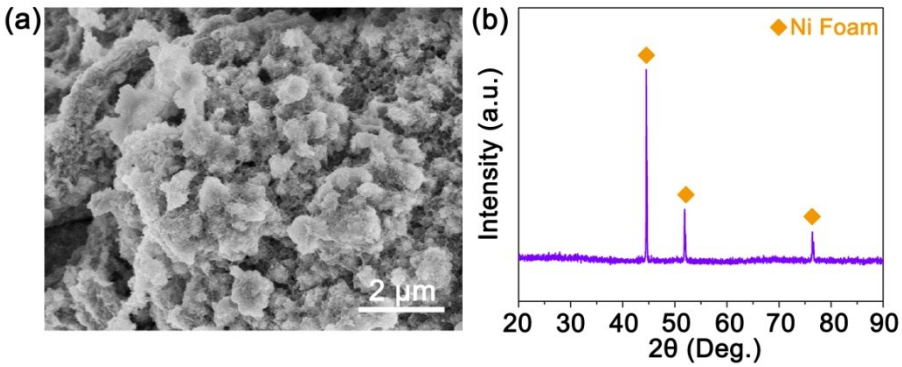

Fig. S6 (a) SEM image and (b) XRD pattern of $Co(OH)_xS$ nanoflakes aggregation.

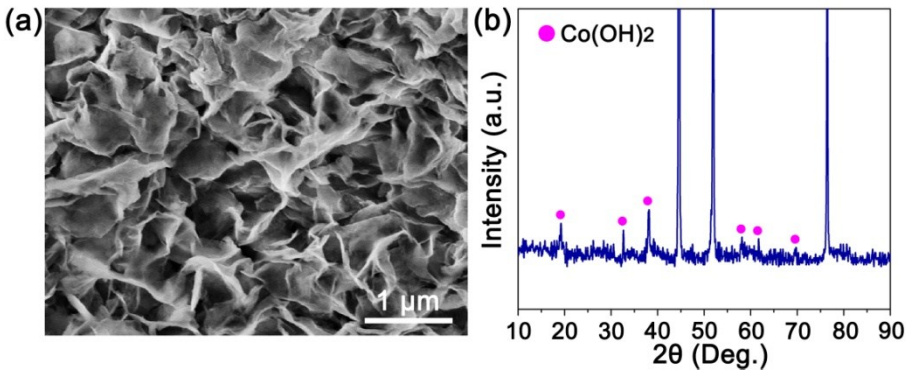

Fig. S7 (a) SEM image and (b) XRD patterns of $Co(OH)_x$ nanoflakes.

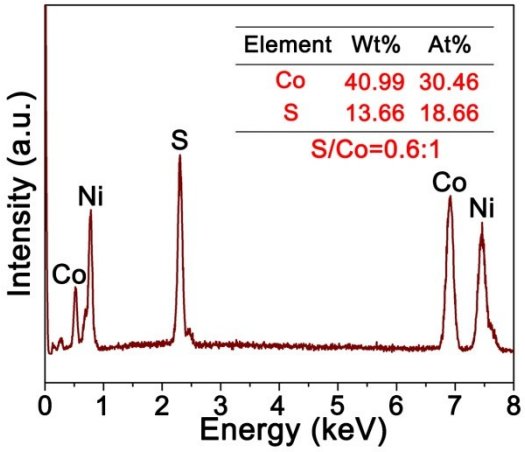

Fig. S8 EDS spectrum of $Co(OH)_xS_{0.6}$ nanoflakes.

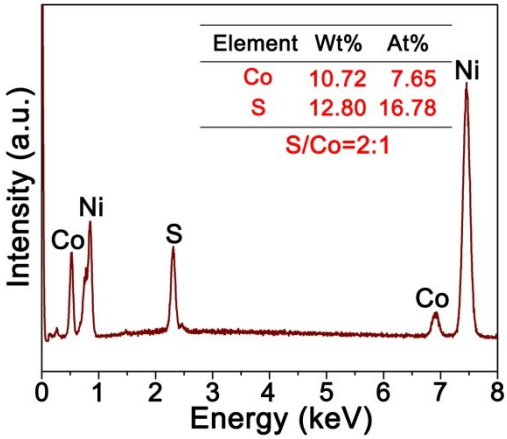

Fig. S9 EDS spectrum of $Co(OH)_xS_2$ nanoflakes.

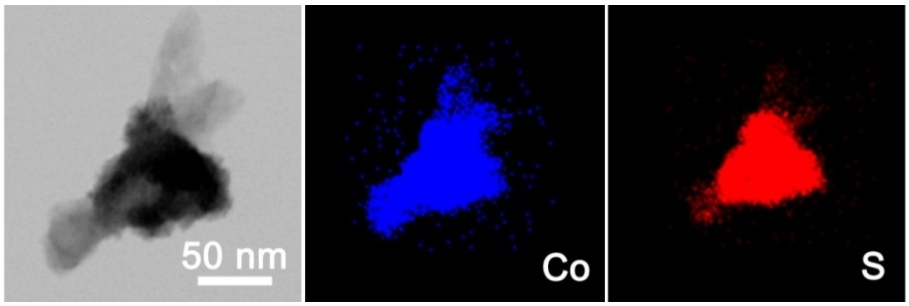

Fig. S10 TEM-EDS mapping of a typical junction in $Co(OH)_xS_2$ nanoflakes.

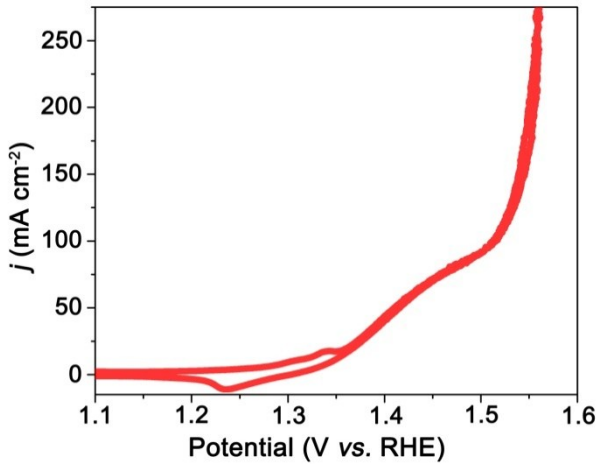

Fig. S11 Cyclic voltammetric curve of $Co(OH)_xS$ nanoflakes at scan rate of 1 mV s^{-1}.

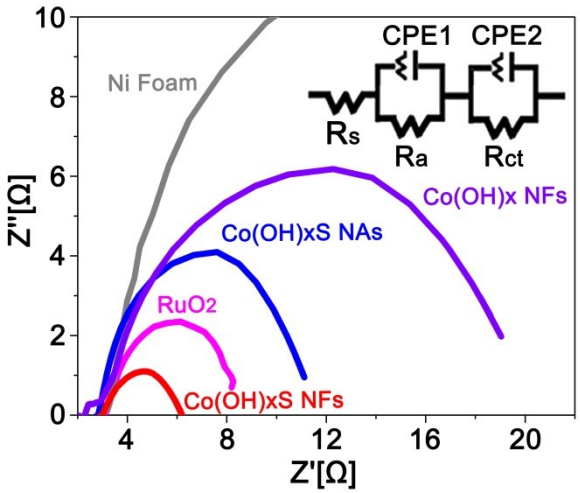

Fig. S12 Nyquist plots of the $Co(OH)_xS$ nanoflakes, the $Co(OH)_xS$ nanoflakes aggregations, the $Co(OH)_x$ nanoflakes and the commercial RuO_2 (*inset* showing the equivalent circuit to fit the data).

The high-frequency response in Nyquist plots can be assigned to the solution resistance (R_s), while the low-frequency response can be assigned to interfacial charge-transfer resistance (R_{ct}) in OER process.

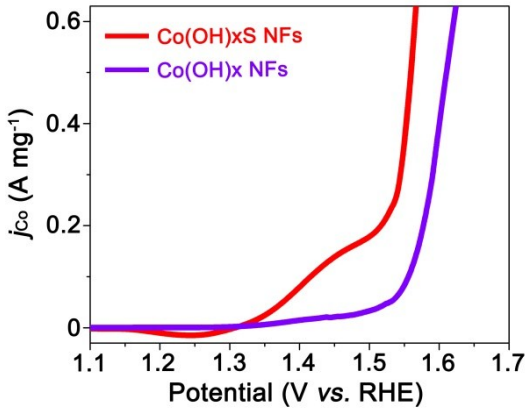

Fig. S13 Mass activity curves of $Co(OH)_xS$ and $Co(OH)_x$ nanoflakes. The calculation is based on the mass loading of Co element.

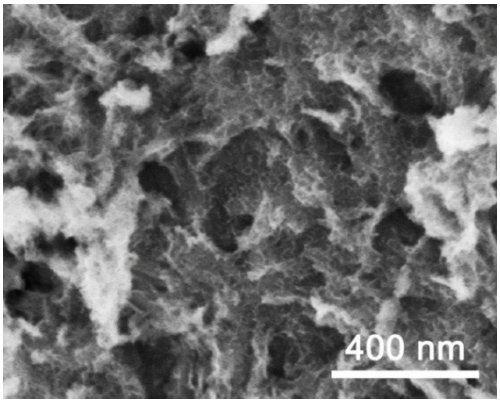

Fig. S14 SEM image of $Co(OH)_xS$ nanoflakes after CP evaluation.

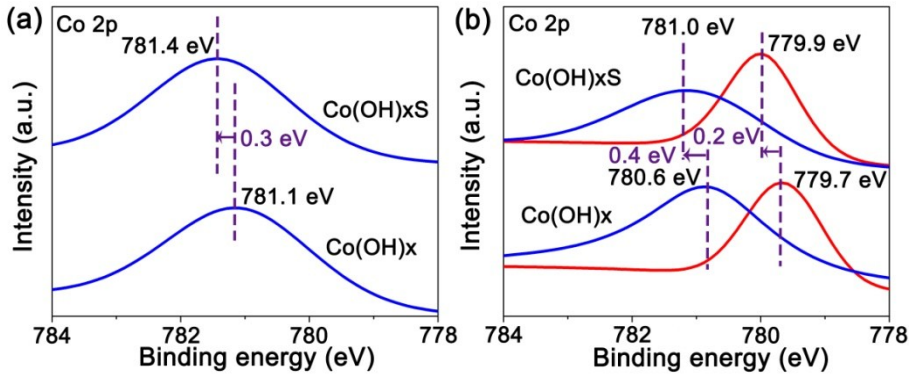

Fig. S15 Co 2p spectra of $Co(OH)_xS$ and $Co(OH)_x$ nanoflakes (a) before and (b) after OER.

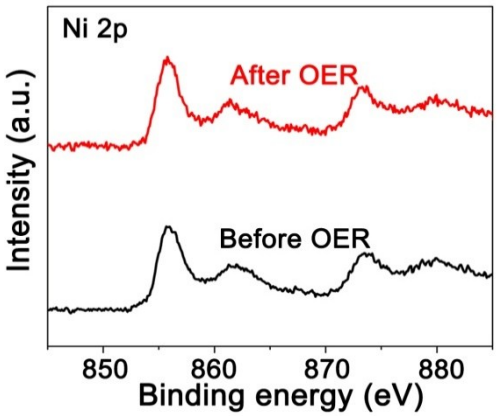

Fig. S16 XPS spectra of Ni 2p region of $Co(OH)_xS$ nanoflakes before and after OER.

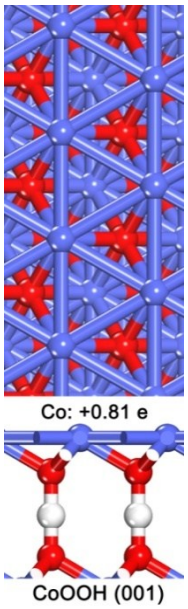

Fig. S17 The optimized model structure of pristine CoOOH (001) facet.

Part III: Supporting Table

Table S1 Comparisons of OER performance of the reported state-of-the-art electrocatalysts.

Electrocatalyst	Mass loading (mg cm^{-2})	Measurement	j (mA cm^{-2})	η (mV)	Tafel slope (mV dec^{-1})	Ref.
MoS_2-Ni_3S_2 nanorods	13.00	Ni foam 1.0 M KOH	100	341	57	23
$Co(OH)_2$ nanoparticle encapsulating conductive nanowires array	7.50	Cu foam 1.0 M KOH	100	330	101	27
Hierarchical Co(OH)F superstructure	/	Glassy carbon 1.0 M KOH	100	390	53	28
$CoFe_2O_4$/C porous hybrid nanorod arrays	1.03	Ni foam 1.0 M KOH	100	285	45	S14
$NiCo_2S_4$ nanowire arrays	/	Ni foam 1.0 M KOH	100	380	40	S15
Co-Mn carbonate hydroxide nanosheets	5.60	Ni foam 1.0 M KOH	100	350	/	S16
FeOOH/CeO_2 nanotubes	0.44	Ni foam 1.0 M KOH	100	320	92	S17
FeOOH/Co/FeOOH nanotube arrays	0.50	Ni foam 1.0 M NaOH	100	> 300	32	S18
NiFe alloyed nanoparticles	1.15	Ni foam 1.0 M KOH	100	290	30	S19
NiS microsphere film	43.00	Ni foam 1.0 M KOH	100	350	89	S20
3D porous Ni_xP_y/Ni	11.04	Ni foam 1.0 M KOH	100	320	73	S21
$Ni_3FeAl_{0.91}$-LDH	0.20	Ni foam 1.0 M KOH	100	350	50	S22
Benzoate intercalated layered $Co(OH)_2$ nanoarray	17.40	Ni foam 1.0 M KOH	100	311	73	S23
Amorphous $Co(OH)_xS$ nanoflakes	1.00	Ni foam 1.0 M KOH	100 200 1000	283 323 365	54	This work

References

S1 G. Kresse, J. Furthmüller, *Phys. Rev. B* 1996, **54**, 11169.

S2 G. Kresse, J. Hafner, *Phys. Rev. B* 1993, **47**, 558.

S3 G. Kresse, J. Hafner, *Phys. Rev. B* 1994, **49**, 14251.

S4 P. E. Blöchl, *Phys. Rev. B* 1994, **50**, 17953.

S5 I. A. Vladimir, F. Aryasetiawan, A. I. Lichtenstein, *J. Phys.: Condens. Matter* 1997, **9**, 767.

S6 V. I. Anisimov, J. Zaanen, O. K. Andersen, *Phys. Rev. B* 1991, **44**, 943.

S7 O. L. Bacq, A. Pasturel, O. Bengone, *Phys. Rev. B* 2004, **69**, 245107.

S8 M. Bajdich, M. García-Mota, A. Vojvodic, J. K. Nørskov, A. T. Bell, *J. Am. Chem. Soc.* 2013, **135**, 13521.

S9 H. J. Monkhorst, J. D. Pack, *Phys. Rev. B* 1976, **13**, 5188.

S10 M. Methfessel, A. T. Paxton, *Phys. Rev. B* 1989, **40**, 3616.

S11 D. Sheppard, R. Terrell, G. Henkelman, *J. Chem. Phys.* 2008, **128**, 134106.

S12 G. Henkelman, A. Arnaldsson, H. Jónsson, *Comput. Mater. Sci.* 2006, **36**, 354.

S13 E. Sanville, S. D. Kenny, R. Smith, G. Henkelman, *J. Comput. Chem.* 2007, **28**, 899.

S14 X. F. Lu, L. F. Gu, J. W. Wang, J. X. Wu, P. Q. Liao, G. R. Li, *Adv. Mater.* 2017, **29**, 1604437.

S15 A. Sivanantham, P. Ganesan, S. Shanmugam, *Adv. Funct. Mater.* 2016, **26**, 4661.

S16 T. Tang, W. J. Jiang, S. Niu, N. Liu, H. Luo, Y. Y. Chen, S. F. Jin, F. Gao, L. J. Wan, J. S. Hu, *J. Am. Chem. Soc.*2017, **139**, 8320.

S17 J. X. Feng, S. H. Ye, H. Xu, Y. X. Tong, G. R. Li, *Adv. Mater.* 2016, **28**, 4698.

S18 J. X. Feng, H. Xu, Y. T. Dong, S. H. Ye, Y. X. Tong, G. R. Li, *Angew. Chem. Int. Ed.* 2016, **55**, 3694.

S19 Y. Feng, H. Zhang, L. Fang, Y. Mu, Y. Wang, *ACS Catal.* 2016, **6**, 4477.

S20 W. X. Zhu, X. Y. Yue, W. T. Zhang, S. X. Yu, Y. H. Zhang, J. Wang, J. L. Wang, *Chem. Commun.* 2016, **52**, 1486.

S21 G. F. Chen, T. Y. Ma, Z. Q. Liu, N. Li, Y. Z. Su, K. Davey, S. Z. Qiao, *Adv. Funct. Mater.* 2016, **26**, 3314.

S22 H. Liu, Y. Wang, X. Lu, Y. Hu, G. Zhu, R. Chen, L. Ma, H. Zhu, Z. Tie, J. Liu, Z. Jin, *Nano Energy* 2017, **35**, 350.

S23 R. Ge, X. Ren, X. Ji, Z. Liu, G. Du, M. Asiri Abdullah, X. Sun, L. Chen, *Chemsuschem* 2017, **10**, 4004.